View metadata, citation and similar papers at core.ac.uk
brought to you by CORE
provided by espace@Curtin

Applied Mathematical Sciences, Vol. 8, 2014, no. 60, 2951 - 2964
HIKARI Ltd, www.m-hikari.com
http://dx.doi.org/10.12988/ams.2014.43204

A New Approach for Modelling Insolation from the Space Perspective

Sofya Prakhova

Department of Mathematics and Statistics, Curtin University
GPO Box U1987, Perth, Western Australia, 6845

Igor Suleimanov

Department of Mathematics, Ufa State Petroleum Technical University
1 Kosmonavtov street, Ufa, Russia, 450062

Volker Rehbock

Department of Mathematics and Statistics, Curtin University
GPO Box U1987, Perth, Western Australia, 6845

Copyright © 2014 Sofya Prakhova, Igor Suleimanov and Volker Rehbock. This is an open access article distributed under the Creative Commons Attribution License, which permits unrestricted use, distribution, and reproduction in any medium, provided the original work is properly cited.

Abstract

In the current project we have developed a novel insolation model which allows users to incorporate the impact of space activity (solar flares, galactic radiation) on the Earth's climate. The incoming radiation was modelled as a flux passing through a cross-section (latitudinal belt), and the changes of light throughout the year were represented by an ellipse with changing parameters. This approach has allowed us to get the results for any latitude at any particular time. Obtained results indicate an average accuracy of 97% with only a few percent less for polar regions.

Keywords: Insolation Modelling, Surface Integrals, External Forces

Introduction

Researchers have been trying to model incoming solar radiation for a long time already, with the first attempts belonging to Milankovitch [4], who first developed a set of formulae for calculating daily insolation. The method was based on spherical trigonometry applied to the astronomical coordinates on the celestial sphere. The English version is available in, for example, [5]. The theory was developed in order to explain the long-term variations in the orbital parameters.

Later on a work was continued by Budyko [2] and Sellers [9], who started the development of simple energy balance models, where some representation of insolation was required. In both works, the annual mean tabulated values for each latitudinal belt were used in order to model insolation reaching the outer boundary of the atmosphere. North in his research [6] also used the mean annual distribution of radiation, but he approximated it by the second Legendre polynomial. His later research [7] includes the seasonal distribution of insolation as well, which was again approximated by the second order Legendre polynomial. At the same time Berger in his paper [1] brought back the attention to the geometry based formulae for computing daily insolation proposed earlier by [4].

These existing modelling approaches are commonly used in current global climate models, such as those described in [3], [8], [10], [11]. However, they cannot incorporate the influence of external forces which can have a big impact on our climate and which may even lead to extreme events. In this paper we aim to model the incoming radiation as a flux coming from space, which will be a good basis for incorporating the impact of space activity in the future. The derivation uses the methods of vector field theory and surface integrals.

Obtained results indicate an average accuracy of 97% with only a few percent less for the regions beyond the polar circles. The chosen modelling approach is sufficiently flexible for incorporating the impact of space activity, such as solar flares, galactic radiation, cross galactic radiation etc.

1. Model description

Consider Figure 1

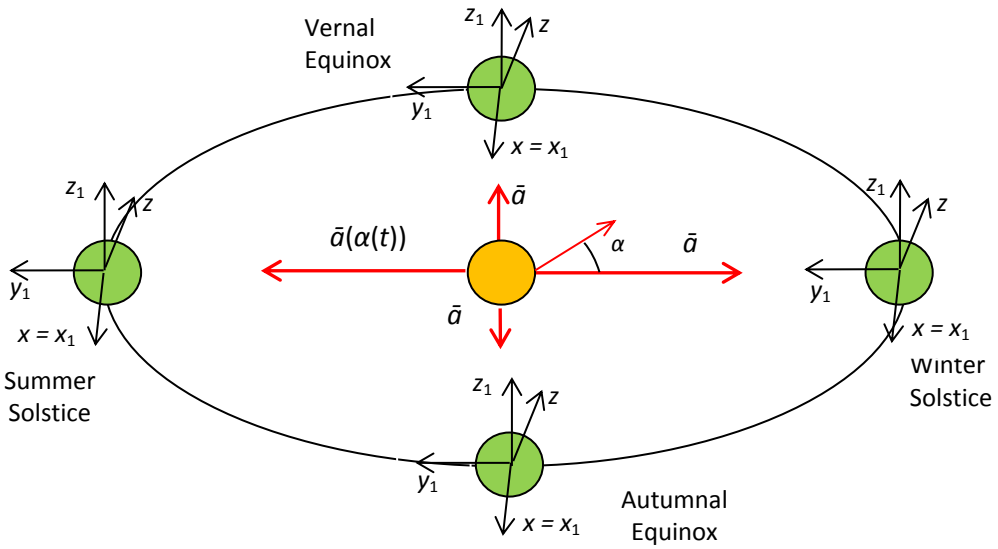

Fig.1. Coordinate systems and radiation vector (annual cycle).

Here the radiation vector is $-\bar{a}(\alpha(t)) = [F\sin(\alpha(t)), -F\cos(\alpha(t)), 0]$, F = 1367 Wt/m^2 is the solar constant, and $\alpha \in [0^\circ, 360^\circ]$ is the angle of the Earth's rotation around the Sun, where α=0 corresponds to the winter solstice. The Earth rotates around the Sun in an anticlockwise direction.

The (x, y, z) coordinate axes are aligned with the equatorial plane. The OZ axis represents the Earth's axis of rotation and OY is in the Earth's equatorial plane. The (x_1, y_1, z_1) axes are aligned with the ecliptic plane and this is inclined to the equatorial plane by an obliquity angle ε = 23°26' under present astronomical conditions. This coordinate system remains fixed as the Earth rotates around the Sun.

All the calculations are performed in the (x_1, y_1, z_1) coordinates. The reason for this choice is that the formulation of the radiation vector $\bar{a}$ remains the same as the Earth rotates around the Sun.

The Y_1OZ_1 plane was chosen for projecting a latitudinal belt in the (x_1, y_1, z_1) coordinate frame. Clearly, the projections obtained in that plane are the easiest for calculations (see Figure 2). The ellipses obtained as the projections of the latitudinal belts in the two other planes (X_1OZ_1 and X_1OY_1) are considerably more difficult to use for computations.

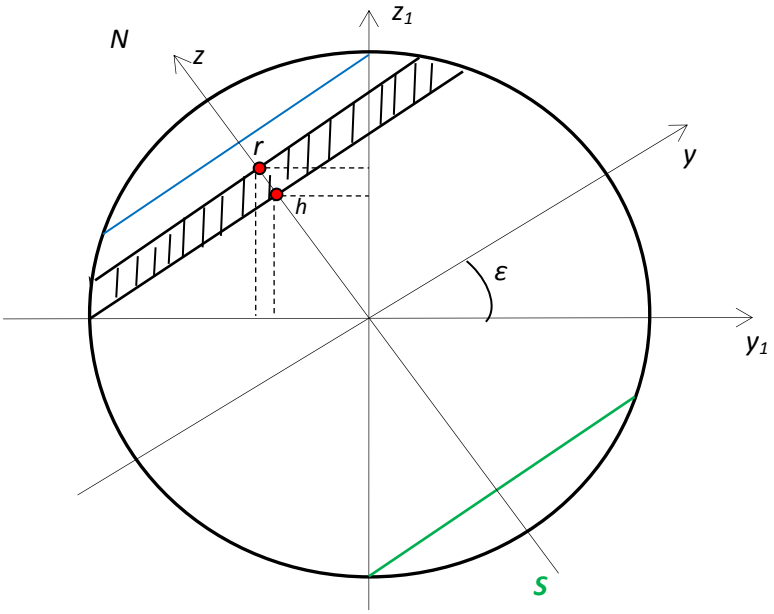

Fig.2. The projection of a latitudinal belt in the chosen projection plane.

In Figure 2, R is the Earth's radius; r and h are the perpendicular distances from the equatorial plane to the upper and lower latitude limits of the belt, respectively.

The direction of radiation vector in the Earth plane and the chosen orientation of the surface are shown in Figure 3.

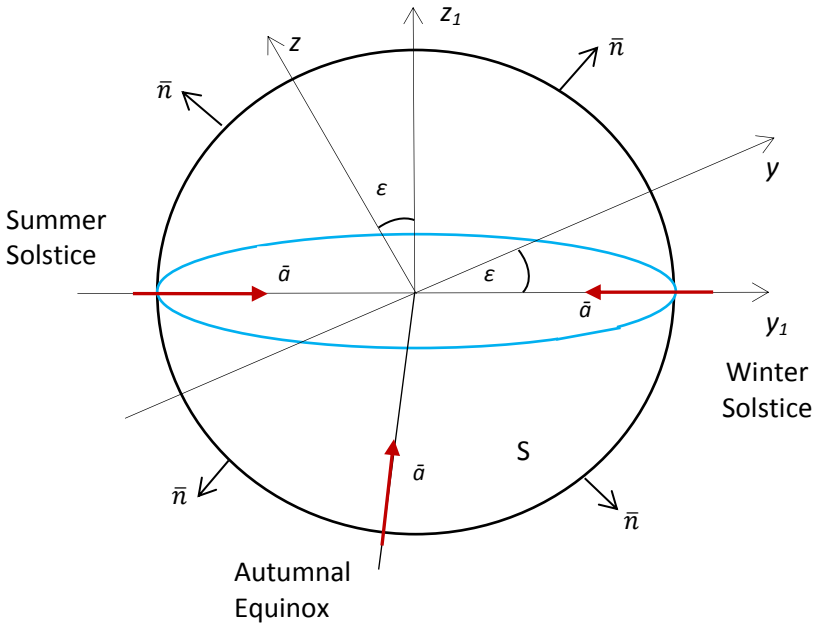

Fig.3. The direction of radiation vector in the Earth plane and the surface orientation.

In Figure 3, $\bar{n}$ denotes the outward unit normal vector.

The positively-oriented surface (S^+) in the chosen projection plane is the part of the sphere closer to the observer. The negatively-oriented surface (S^-) is the part of the sphere pointing away from the observer.

The amount of light which is received by any particular area changes throughout the year. In the current approach it was modelled by an ellipse which changes with time since it has been determined by α (see Figure 4). An ellipse change affects the change of size of the hatched area of the latitudinal belt. This area is referred to as the illumination area from this point onwards. The equations of the ellipse, circle, equator line and upper and lower latitudes are presented in terms of the notations used (see Figure 4).

Sunlight is received by both sides of the surface. However, for computational simplicity this needs to be split into two parts. The illumination area for the positively-oriented surface and for the negatively-oriented surface is introduces in Figure 4.

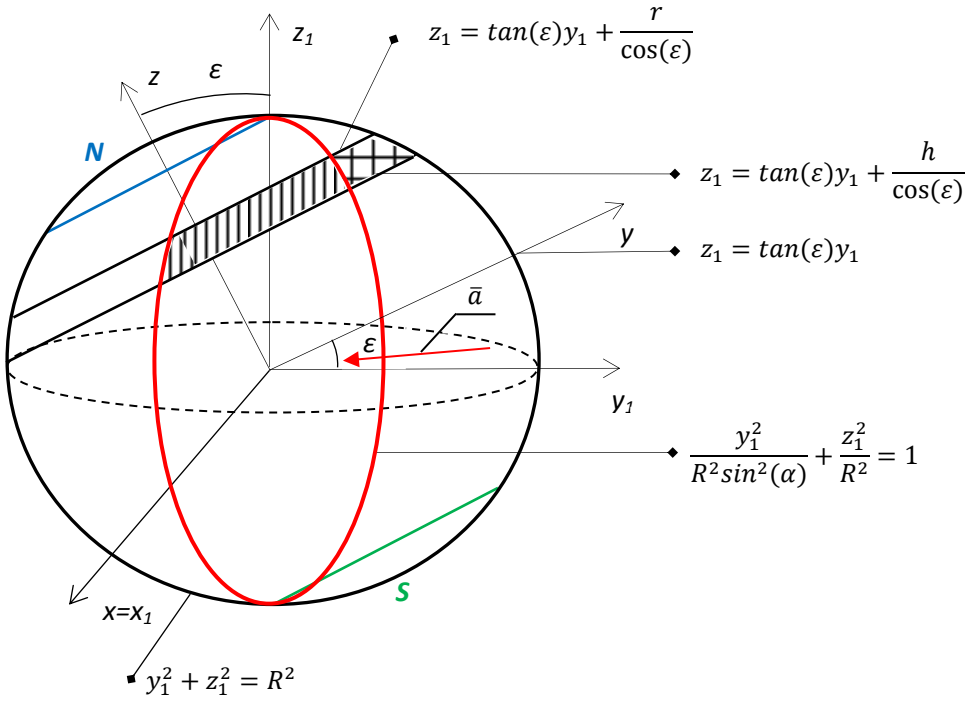

Fig.4. The illumination area for the positively-oriented and for the negatively-oriented surface of the latitudinal belt.

In Figure 4, the forward- hatched illumination area is on the negatively-oriented surface, so it is a strip coming from the side located further from the observer (D^-). The back- hatched illumination area is on the positively-oriented surface, which is a small piece on the side located closer to the observer (D^+).

An example of the illumination area changing as time progresses for the equatorial latitudinal belt (10°-20°) is shown in Figure 5.

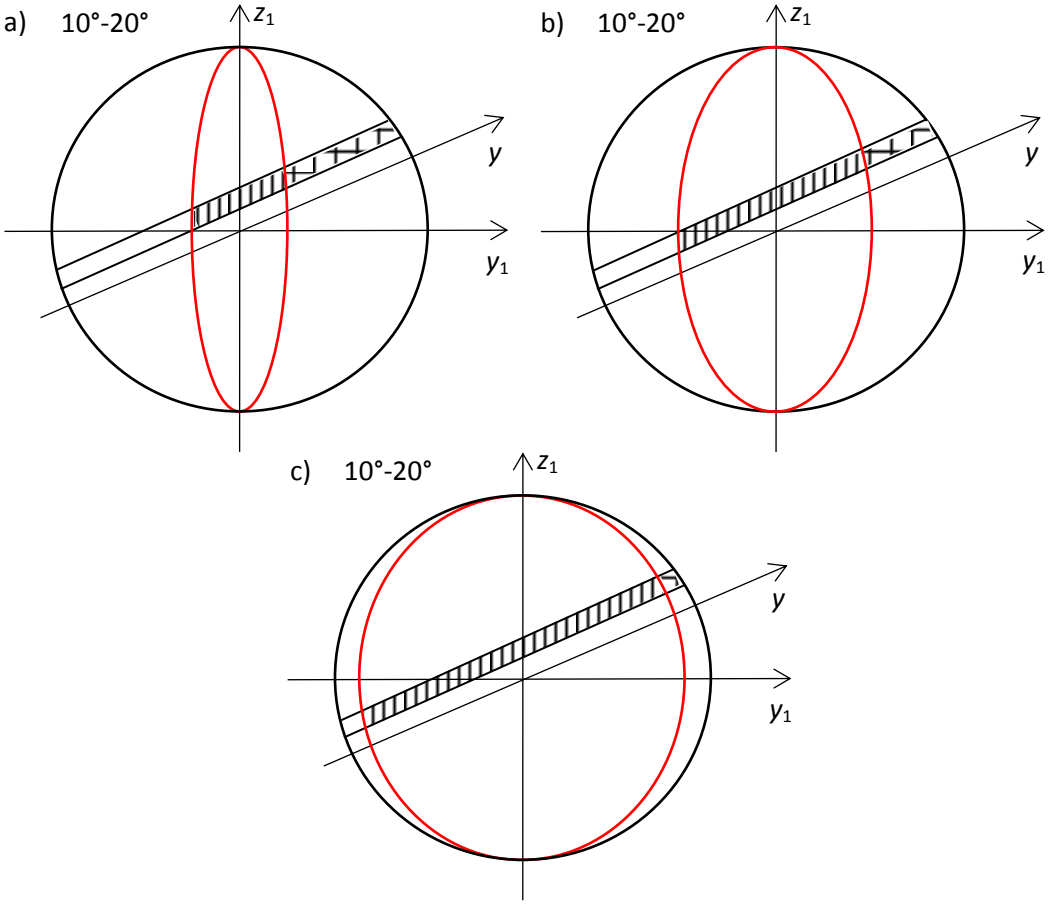

Fig.5. Illumination area change for 10°-20° latitudinal belt for the different moments of time between the winter solstice and the vernal equinox (a-c).

For the latitudes beyond the polar circles the phenomena of polar night and polar day can be observed. This has also been incorporated into modelling. An example is shown in Figure 6.

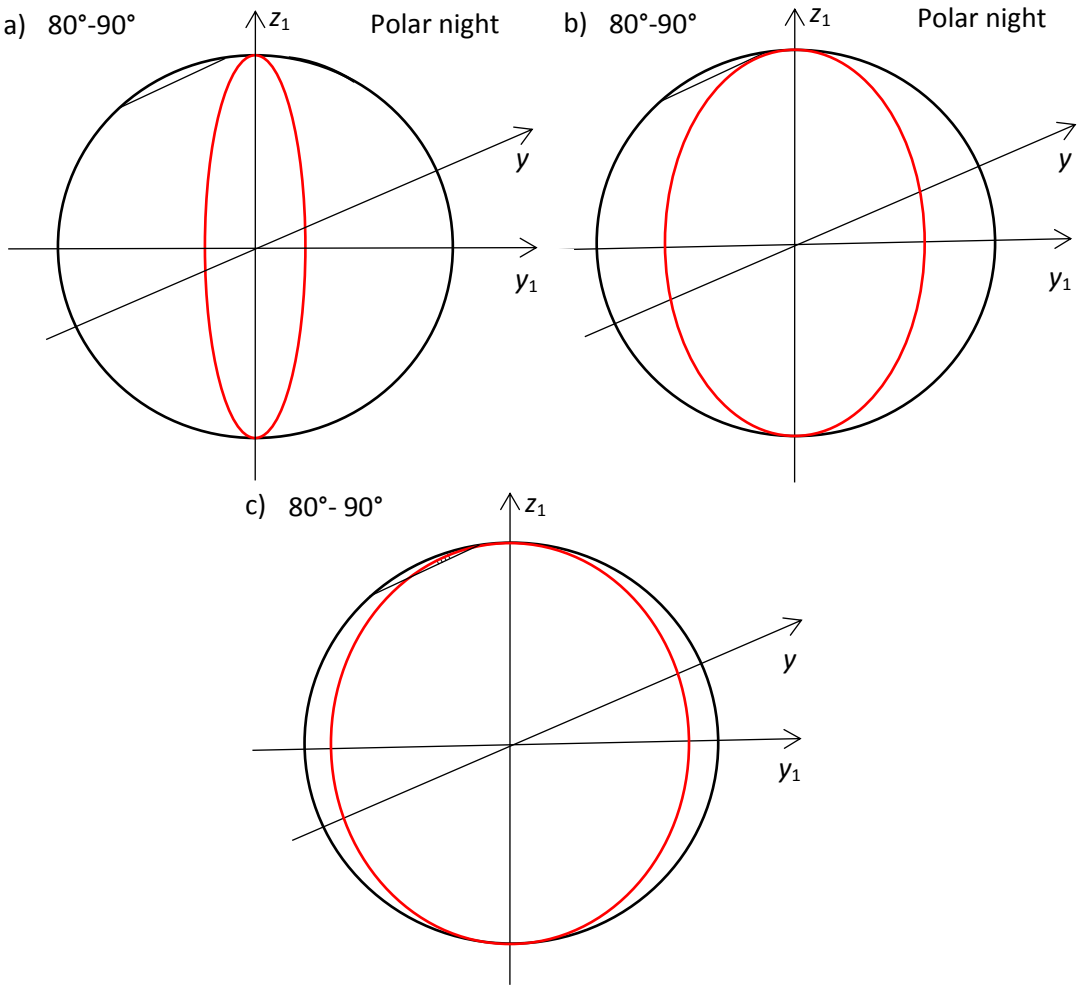

Fig.6. Illumination area change for the 80°-90° latitudinal belt for the different moments of time between the winter solstice and the vernal equinox (a-c).

For the Southern Hemisphere the illumination areas below the equator need to be considered. However, for computational simplicity the symmetrical areas in the Northern Hemisphere were used for calculations. One example is shown in Figure 7.

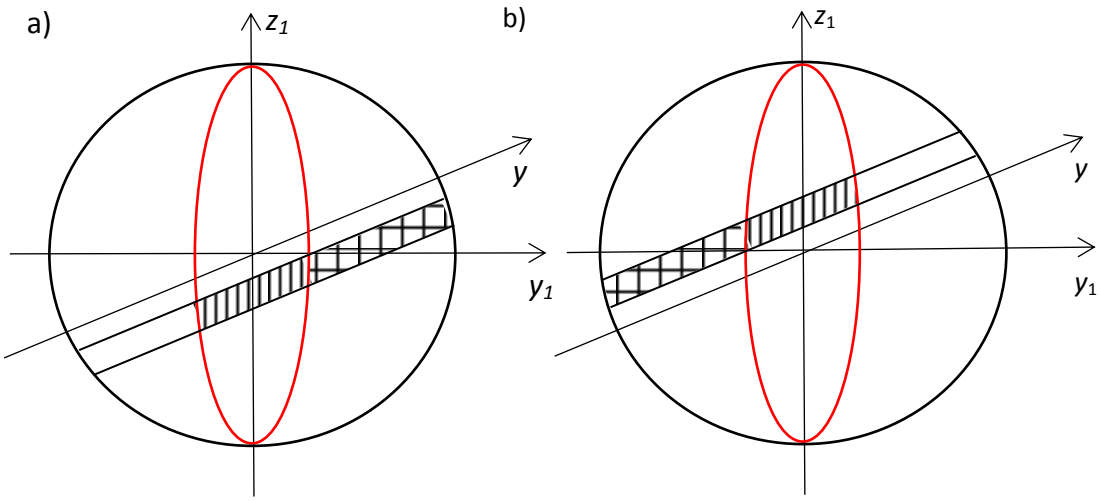

Fig.7. An example of actual illumination area for latitudinal belt in Southern Hemisphere (a) and a symmetrical one in the Northern Hemisphere used for calculation (b)

2. Radiation Calculations

The amount of radiation received per m^2 in the current latitudinal belt (daily average) is the total amount of radiation divided by the surface area of latitudinal belt: $I=Flux/S_{belt}$.

The radiation flux through the surface can be calculated as the product of the radiation vector ($\bar{a}$) and the outward unit normal vector ($\bar{n}$) to the surface (S) integrated over the chosen side of the surface (see Figure 2):

$$Flux = \iint_S (\bar{a} \cdot \bar{n}) dS \tag{1}$$

This can also be written in coordinate form. In order to calculate the flux, the integral was separated into an integral over the positively-oriented surface and an integral over the negatively-oriented surface.

$$Flux = \iint_S (\bar{a} \cdot \bar{n}) dS = \iint_S ax_1 dy_1 dz_1 + ay_1 dx_1 dz_1 + az_1 dx_1 dy_1 = \iint_{S^+} ax_1 dy_1 dz_1 +$$

$$+ ax_1 dy_1 dz_1 + az_1 dx_1 dy_1 + \iint_{S^-} ax_1 dy_1 dz_1 + ay_1 dx_1 dz_1 + az_1 dx_1 dy_1 \tag{2}$$

For the positively-oriented surface (S^+) and for the negatively-oriented surface (S^-) a surface integral was calculated as a double integral over the illumination area. The equation of the sphere ($x_1^2+y_1^2+z_1^2=R^2$) was used as the equation of the surface.

$$\iint_{S^+} ax_1dy_1dz_1 + ay_1dx_1dz_1 + az_1dx_1dy_1 = \iint_{D^+} (F\sin\alpha - F\cos\alpha \cdot \frac{\partial x_1}{\partial y_1})dy_1dz_1 =$$

$$= F\sin\alpha - F\cos\alpha \int_{z_1\alpha}^{z_1\beta} dz_1 \int_{y_1\alpha}^{y_1\beta} \frac{y_1}{\sqrt{R^2 - y_1^2 - z_1^2}} dy_1 \quad (3)$$

$$\iint_{S^-} ax_1dy_1dz_1 + ay_1dx_1dz_1 + az_1dx_1dy_1 = \iint_{D^-} (F\sin\alpha - F\cos\alpha \cdot \frac{\partial x_1}{\partial y_1})dy_1dz_1 =$$

$$= F\sin\alpha + F\cos\alpha \int_{z_1\alpha}^{z_1\beta} dz_1 \int_{y_1\alpha}^{y_1\beta} \frac{y_1}{\sqrt{R^2 - y_1^2 - z_1^2}} dy_1 \quad (4)$$

Here $z_1\alpha$, $y_1\alpha$ and $z_1\beta$, $y_1\beta$ are the lower and upper limits of integration, respectively. These limits are derived from the equations shown in Figure 4.

The projection of a latitudinal belt in *YOZ* plane and *XOY* plane are shown in Figure 8.

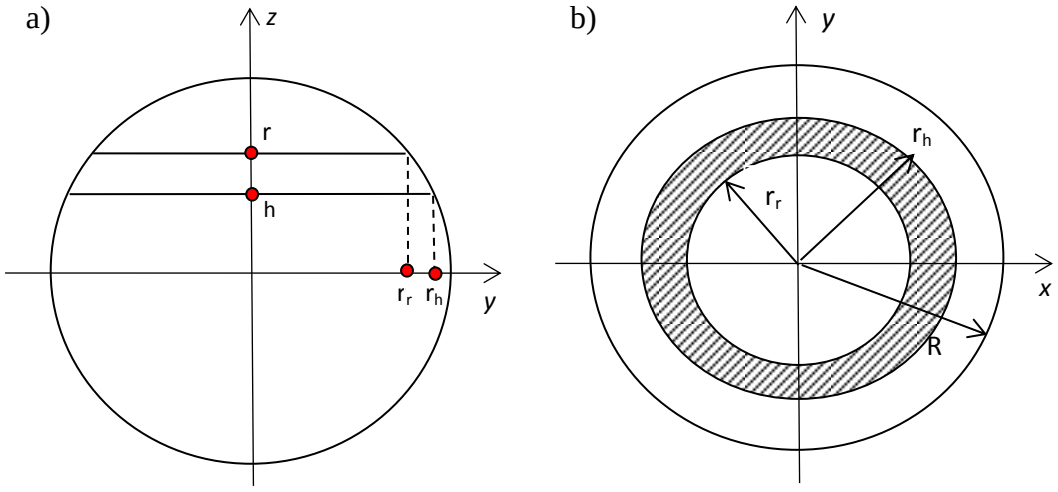

Fig.8. The projection of latitudinal belt in *YOZ* plane (a) and *XOY* plane (b).

For computational simplicity the calculations were performed in the *XOY* plane. The latitudinal belt area was calculated as follows:

$$S_{belt} = \iint_D \sqrt{1+(\frac{\partial z}{\partial x})^2+(\frac{\partial z}{\partial y})^2}\,dxdy = \iint_D \frac{R}{R^2-x^2-y^2}\,dxdy =$$
$$= R\int_0^{2\pi} d\varphi \int_{r_r}^{r_h} \frac{\rho d\rho}{\sqrt{R^2-\rho^2}} = 2\pi R(r-h) \qquad (5)$$

Here $z=\sqrt{R^2-x^2-y^2}$, $r_r=\sqrt{R^2-r^2}$ and $r_h=\sqrt{R^2-h^2}$ (see Figure 8a) are the radii of upper and lower limits of the belt, respectively.

In order to determine the amount of radiation per square metre (*I*), the surfaces of the belt and the double integrals were calculated for each latitudinal belt of a width of 10° for the Northern and Southern Hemisphere using the Maple software. The time step for α was chosen to be 10° (~10 days).

The calculations were performed for the period of time from the winter solstice to the spring equinox. This corresponds to the first quadrant of the circle starting from the winter solstice (α=0°) and going anticlockwise (see Figure 1) to the vernal equinox (α=90°).

Thus a set of nine radiation values has been obtained for both Hemispheres, further referred to as N (0°-90°) and S (0°-90°). The amount of radiation per square metre (*I*) for the rest of the year was obtained as shown in Table 1 by combining these sets and rearranging the data in them.

Table 1. Calculations of the insolation for the whole year period for Northern Hemisphere and Southern Hemisphere

Quadrant of circle and the corresponding period of time	Radiation values	
	Northern Hemisphere	Southern Hemisphere
I (winter solstice-vernal equinox)	N (0°-90°)	S (90°-0°)
II (vernal equinox-summer solstice)	S (0°-90°)	N (90°-0°)
III (summer solstice-autumnal equinox)	S (0°-90°)	N (0°-90°)
IV (autumnal equinox-winter solstice)	N (90°-0°)	S (90°-0°)

Note also that it is easy to modify the procedure for thinner belts for more accuracy.

3. Results

The amount of insolation for a complete year cycle for the Northern and Southern Hemisphere are shown in Figures 9-10.

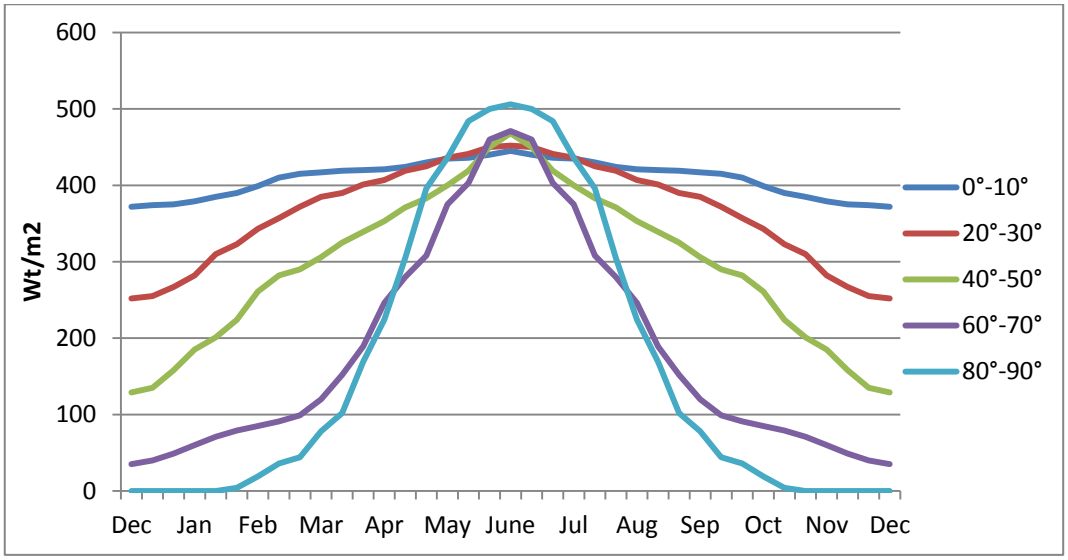

Fig.9. The amount of radiation received for different latitudinal belts in the Northern Hemisphere.

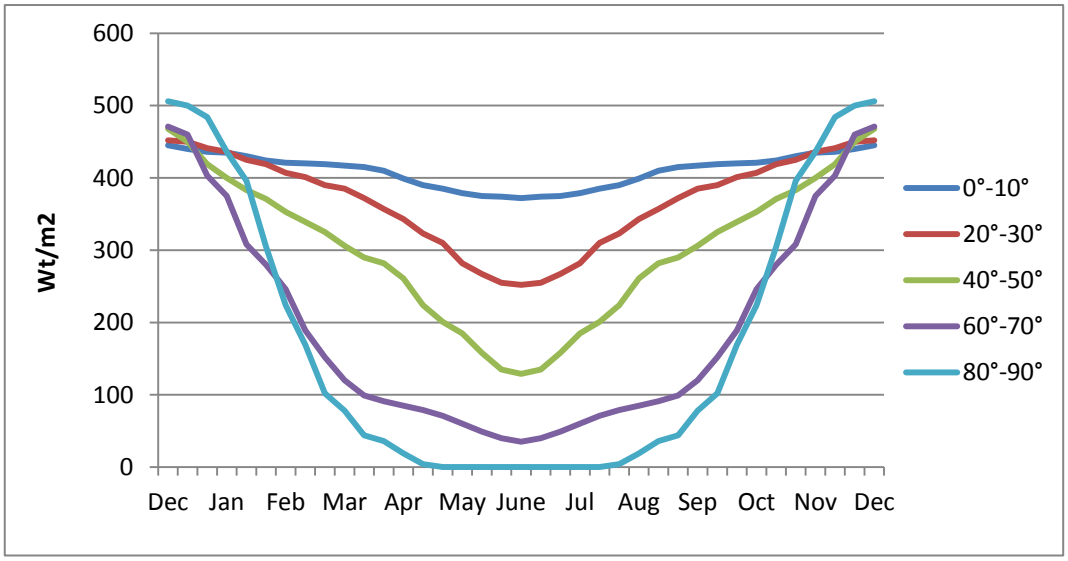

Fig.10. The amount of radiation received for different latitudinal belts in the Southern Hemisphere.

Note that smoother curves would result from using a smaller step size for α.

In Table 2, we also calculate the annual average value for each latitudinal belt and compare it with satellite data [12]. These data were obtained from the NASA Langley Research Center Atmospheric Science Data Center Surface meteorological and Solar Energy (SSE) web portal supported by the NASA LaRC POWER Project. Note that the data from [12] is given in terms of 1° resolution. In Table 2, we have averaged this over the 10° latitudinal belts.

Table 2. Comparison of the obtained results with satellite data

Latitudinal belt	Satellite data (Wt/m^2)	Proposed model (Wt/m^2)	Accuracy
0°-10°	415.00	410.00	0.99
10°-20°	398.45	387.50	0.97
20°-30°	378.29	376.20	0.99
30°-40°	359.76	346.50	0.99
40°-50°	304.33	300.83	0.99
50°-60°	257.78	251.33	0.97
60°-70°	220.00	213.22	0.97
70°-80°	182.02	172.50	0.95
80°-90°	169.89	159.17	0.94
Average			0.97

The obtained results indicate a very good agreement in modelling the annual distribution of insolation for the equatorial and middle latitude regions (average accuracy of 98%). Slightly less agreement can be observed for the polar regions (94.5%). The average accuracy of the model is 97%.

4. Discussion and Conclusions

In the current project the amount of insolation reaching the outer boundary of the atmosphere for any latitude at any particular time has been modelled. This has yielded excellent results with an average accuracy of the model being 97%.

We should note the Earth was assumed to be exactly spherical. In addition, small variations in the distance between the Sun and the Earth while it travels on it orbit have not been considered in our proposed model so far. However, this effect is very small and can be easily incorporated in the future.

In the current paper a new approach for modelling the process of receiving radiation by Earth has been introduced. This time this process has been modelled from the space perspective, while all the existing models use the Earth's point of view. This new approach provides an opportunity to incorporate the influence of space activity, which can have a significant impact on the Earth's climate.

In addition, since the proposed model is fully-analytic, it gives the opportunities to capture possible variations in all of the input parameters (such as obliquity, solar constant) and to investigate their impact on climate.

References

[1] A.L. Berger, Long-term variations of daily insolation and quaternary climatic changes, Journal of the Atmospheric Sciences, **35** (1978), 2362-2367.

[2] M. Budyko, The effect of solar radiation variations on the climate of the Earth, *Tellus*, **21** (1969), 611-619.

[3] K. Matsumoto, K.S. Tokos, A. Price, and S. Cox, First description of the Minnesota Earth System Model for Ocean biogeochemistry (MESMO 1.0), Geoscientific Model Development, **1** (2008), 1-15. 10.5194/gmd-1-1-2008

[4] M. Milankovitch, Théorie mathématique des phénomènes thermiques produits par la radiation solaire, Paris, 1920.

[5] M. Milankovič, Canon of insolation and the ice-age problem, Zavod za udžbenike i nastavna sredstva, 1998.

[6] G.R. North, Analytical solution to a simple climate model with diffusive heat transfer, Journal of the Atmospheric Sciences, **32** (1975), 1301-1307.

[7] G. R. North and J. A. Coakley Jr, Differences between seasonal and mean annual energy balance model calculations of climate and climate sensitivity, Journal of the Atmospheric Sciences, **36 (7)** (1979), 1189-1204.

[8] S.P. Ritz, T.F. Stocker, F. Joos, A Coupled Dynamical Ocean–Energy Balance Atmosphere Model for Paleoclimate Studies, Journal of Climate, **24** (2011), 349–375. http://dx.doi.org/10.1175/2010JCLI3351.1

[9] W. Sellers, A global climatic model based on the energy balance of the earth-atmosphere system, *Journal of Applied Meteorology*, **8** (1969), 392-400.

[10] G. Shaffer, S. Malskær Olsen and J.O. Pepke Pedersen, Presentation, calibration and validation of the low-order, DCESS Earth System Model (Version 1), Geoscientific Model Development, **1** (2008), 17-51. 10.5194/gmd-1-17-2008

[11] A.J. Weaver et al., The UVic earth system climate model: Model description, climatology, and applications to past, present and future change, Atmosphere-Ocean, **39 (4)** (2001), 361-428.

[12] https://eosweb.larc.nasa.gov/sse/global/text/22yr_toa_dwn, accessed 10.06.2013

Received: March 21, 2014